

Echo-Planar Imaging of Porous Media with Spatial Resolution below $100\ \mu\text{m}$

B. Manz, P. S. Chow, and L. F. Gladden

Department of Chemical Engineering, University of Cambridge, Pembroke Street, Cambridge CB2 3RA, United Kingdom

Received July 14, 1998; revised September 9, 1998

A modified version of the echo-planar imaging technique incorporating a Carr–Purcell train of 180° rf pulses (PEPI) has been implemented on a standard spectrometer. It is demonstrated that artifacts in the image due to cumulative errors in the rf field can be reduced by replacing each 180° pulse by a composite sequence of three rf pulses. Artifact-free 3D images at $94\ \mu\text{m}$ voxel resolution are obtained within 15 min. This technique has been applied to study the drying process in an initially water-saturated model porous medium with characteristic T_2^* of order $700\ \mu\text{s}$. © 1999

Academic Press

Key Words: EPI; porous media; composite pulses.

Magnetic resonance imaging (MRI) techniques are now established as a probe of the spatially resolved distribution of physical properties in porous media. For example, a three-dimensional volume image of the fluid density distribution filling the pore space can be analyzed to obtain characteristics of the void space and of the individual pores within the pore space (1, 2). Of increasing interest is the application of MRI to follow dynamic processes in such systems at high resolution and in three dimensions. An important issue is therefore the time scale for signal acquisition; steady-state conditions within the sample are required on a time scale defined by the acquisition time for one image. Using the spin-echo method, the acquisition of a single two-dimensional image is on the order of minutes, while a full three-dimensional image takes several hours. With high-speed imaging techniques it is possible to obtain a two-dimensional image in less than one second. In particular, echo-planar imaging (EPI) (3) allows the acquisition of a full two-dimensional image from one single excitation. However, in porous media the variation of magnetic susceptibility gives rise to a rapid T_2^* relaxation, which leads to serious distortions and blurring in the EPI images. PEPI (π -EPI) (4, 5) is a modification of EPI, where the gradient reversals are replaced by unipolar gradient pulses centered around a 180° rf pulse. These 180° rf pulses refocus the magnetization, which is dephased by magnetic field inhomogeneities. Due to these 180° rf pulses, the k -space trajectory is different from EPI, and the echoes have to be reordered prior to Fourier transformation (4). Based on this method is a PEPI hybrid, which allows the acquisition of a full three-dimensional image within several minutes (6). The PEPI experiment is related to the RARE

(rapid acquisition with relaxation enhancement) experiment, which also uses a train of spin echoes for fast image acquisition (7, 8). In this paper we demonstrate how PEPI and the PEPI hybrid can be implemented on a standard spectrometer with a microimaging facility. No modifications to the hardware are necessary.

The three-dimensional PEPI hybrid pulse sequence is shown in Fig. 1. If all refocusing pulses have the same phase, unwanted transverse magnetization due to imperfect rf pulses causes a central line artifact in the image. By alternating the phase of the refocusing pulses in a two-step x , y phase cycle, this artifact can be reduced in intensity and shifted to the edge of the image (9). Such a phase cycle has been suggested by Gullion *et al.* for the compensation of cumulative pulse errors in Carr–Purcell sequences. Further improvement may be achieved by using a more complex 16-step phase cycle consisting of x and y pulses (10).

A different approach to compensating for pulse errors in spin-echo experiments is the use of composite rf pulses (11). If the refocusing pulse $R_y(\pi)$ of a Carr–Purcell sequence is replaced by a composite sequence of three rf pulses, $R_x(\pi/2)R_y(\pi)R_x(\pi/2)$, good spin-state inversion is achieved even for pulses with a flip angle different from 180° , but there is a phase shift Δ between even-numbered and odd-numbered echoes. Using the PEPI sequence shown in Fig. 1, the value of Δ can be obtained by a comparison of the first two echoes. An automatic phasing algorithm is used to calculate Δ . This value of Δ is then used to correct all odd-numbered echoes prior to Fourier transformation. For *in vivo* applications it is important to note that the rf power deposition is increased fourfold using such a sequence of composite pulses.

Both the two-dimensional PEPI and the three-dimensional PEPI hybrid were implemented on a standard Bruker DMX 200 spectrometer with actively shielded microimaging gradients. The receiver was left open during the entire Carr–Purcell train in order to enable a rapid acquisition. The individual echoes were subsequently rearranged using the data rearrangement procedures given in Refs. (4, 6). In order to avoid magnetic field gradients induced by eddy currents due to the fast switching of the gradients, the read gradient was ramped in 100 steps of $0.5\ \mu\text{s}$ duration between zero and the maximum value, as shown in Fig. 1. One hundred twenty-eight echoes were

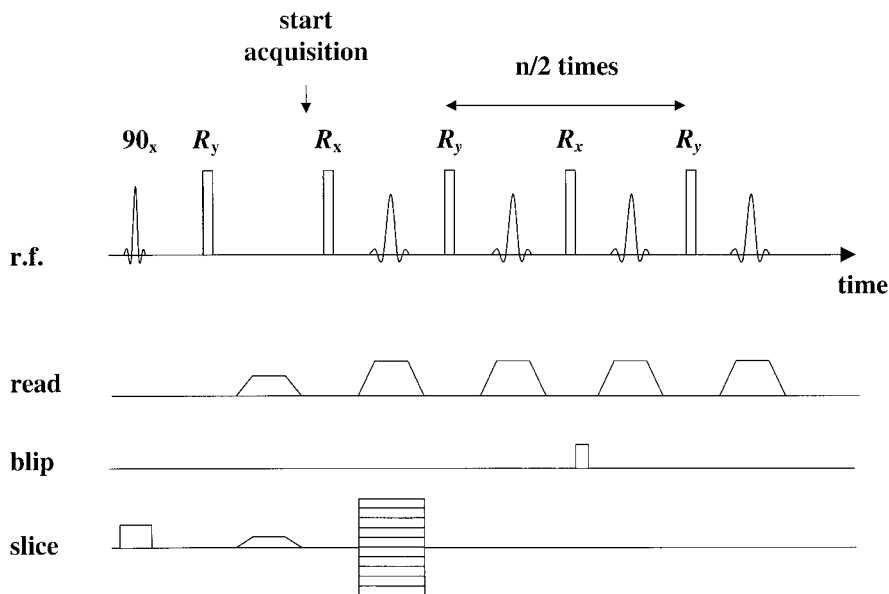


FIG. 1. Pulse-timing diagram for the three-dimensional PEPI hybrid sequence (6). A CPMG train of 180° rf pulses is applied in the gaps between the read gradient pulses. Cumulative errors in the rf field can be refocused by replacing the refocusing pulses R_x and R_y by composite pulses, as described in the text.

acquired, each echo consisting of 128 complex data points with a dwell time of $5 \mu\text{s}$. The duration of the blip gradient was $500 \mu\text{s}$, and the time for one echo was 3.28 ms, giving a total acquisition time of 420 ms for one scan. An important issue is the effect of T_2 relaxation and self-diffusion during the acquisition time on spatial resolution. Observation of the echo signal with no blip gradients applied showed that the amplitude of the final echo was attenuated to approximately 30% compared to the first echo. This leads to a smoothing of the images in the phase direction. However, this smoothing effect is small (less than 10%) compared to the smoothing introduced by the \sin^2 apodization filter, which has been applied to both spin-echo and PEPI images.

The pulse sequences were tested on a model porous medium

sample consisting of a packed bed of glass spheres (1.0 mm diameter) inside a 10-mm-diameter glass tube. The pore space was filled with deionized water. Figure 2 shows a spin-echo image (a) and a PEPI image (b) of a transverse slice of thickness 0.5 mm through the sample. Eight transients were acquired for signal averaging with a repetition time of 3 s, giving a total experiment time of 51 min for the spin-echo experiment, compared to 24 s for the PEPI experiment. The effect of rf pulse errors becomes evident from the three-dimensional image, of which two orthogonal slices through the central section are shown in Fig. 3. The spin-echo image shown in Figs. 3a and 3b was acquired by taking two signal averages with a repetition time of 1 s and 128^2 phase steps, corresponding to a total experiment time of 9 h. The PEPI images shown

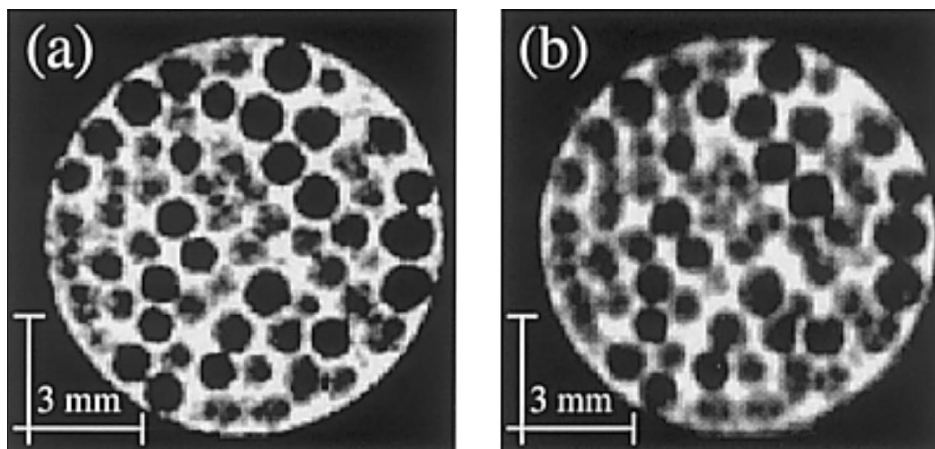


FIG. 2. A two-dimensional spin-echo (a) and PEPI (b) image of the water distribution in a transverse slice through a packed bed of 1.0-mm glass spheres. The pixel resolution is $94 \mu\text{m}$ with a slice thickness of 0.5 mm.

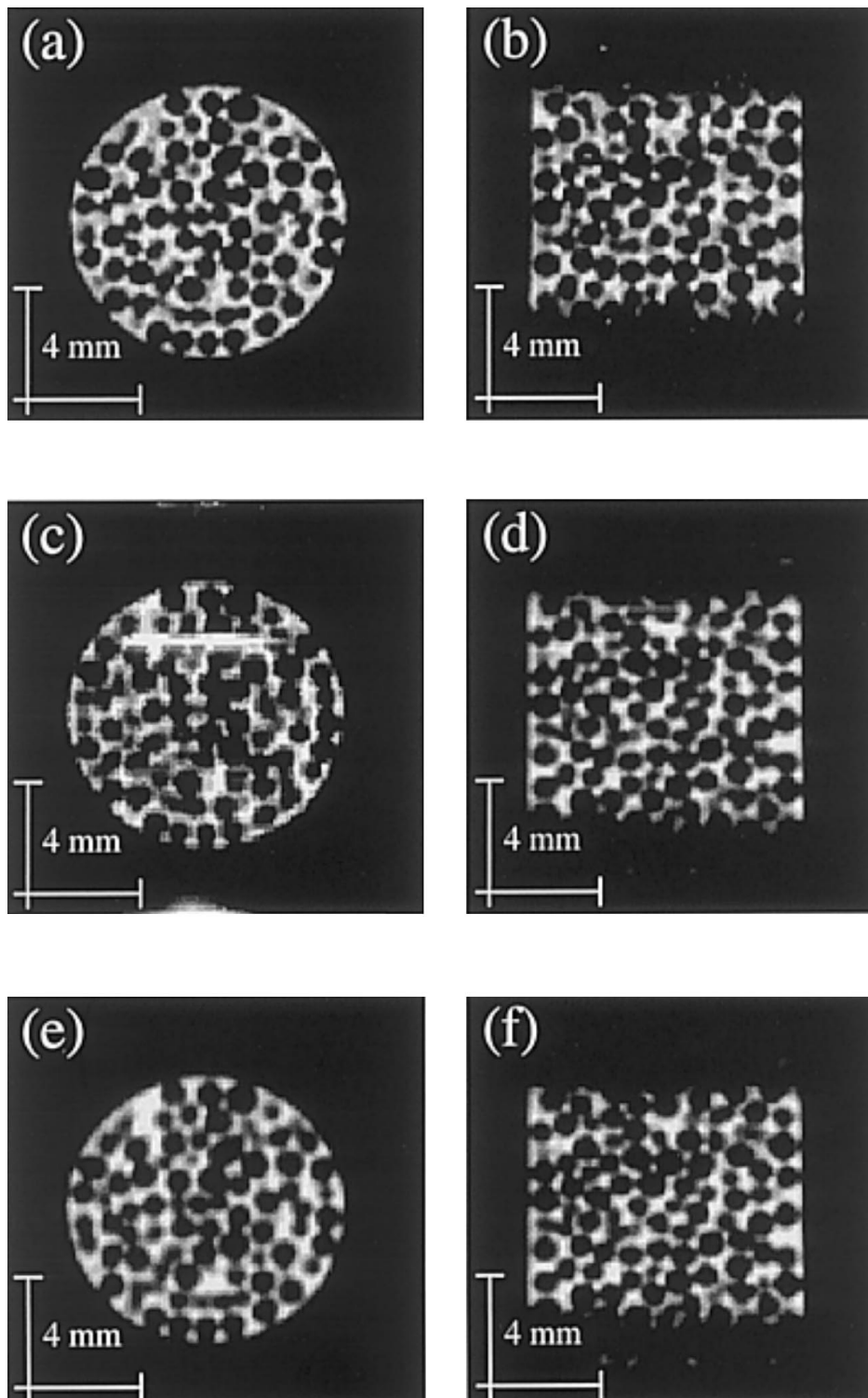


FIG. 3. Two images of orthogonal slices showing the water distribution in a packed bed of 1.0-mm glass spheres. Images (a), (b) were recorded using a three-dimensional spin-echo pulse sequence, while (c), (d) and (e), (f) were recorded using the three-dimensional PEPI hybrid without and with composite refocusing rf pulses, respectively. Note the ghosting artifacts in (c) due to errors in the rf field. The voxel resolution is $117 \mu\text{m}$.

in Figs. 3c–3f were acquired by taking two signal averages with a repetition time of 3.5 s and 128 phase steps, corresponding to a total experiment time of 15 min. Figures 3c and 3d show two orthogonal slices through the three-dimensional im-

age acquired using the PEPI hybrid with a two-step x , y phase cycling in the Carr–Purcell train, while in Figs. 3e and 3f composite 180° rf pulses and a two-step x , y phase cycling in the Carr–Purcell train were used. The agreement between the

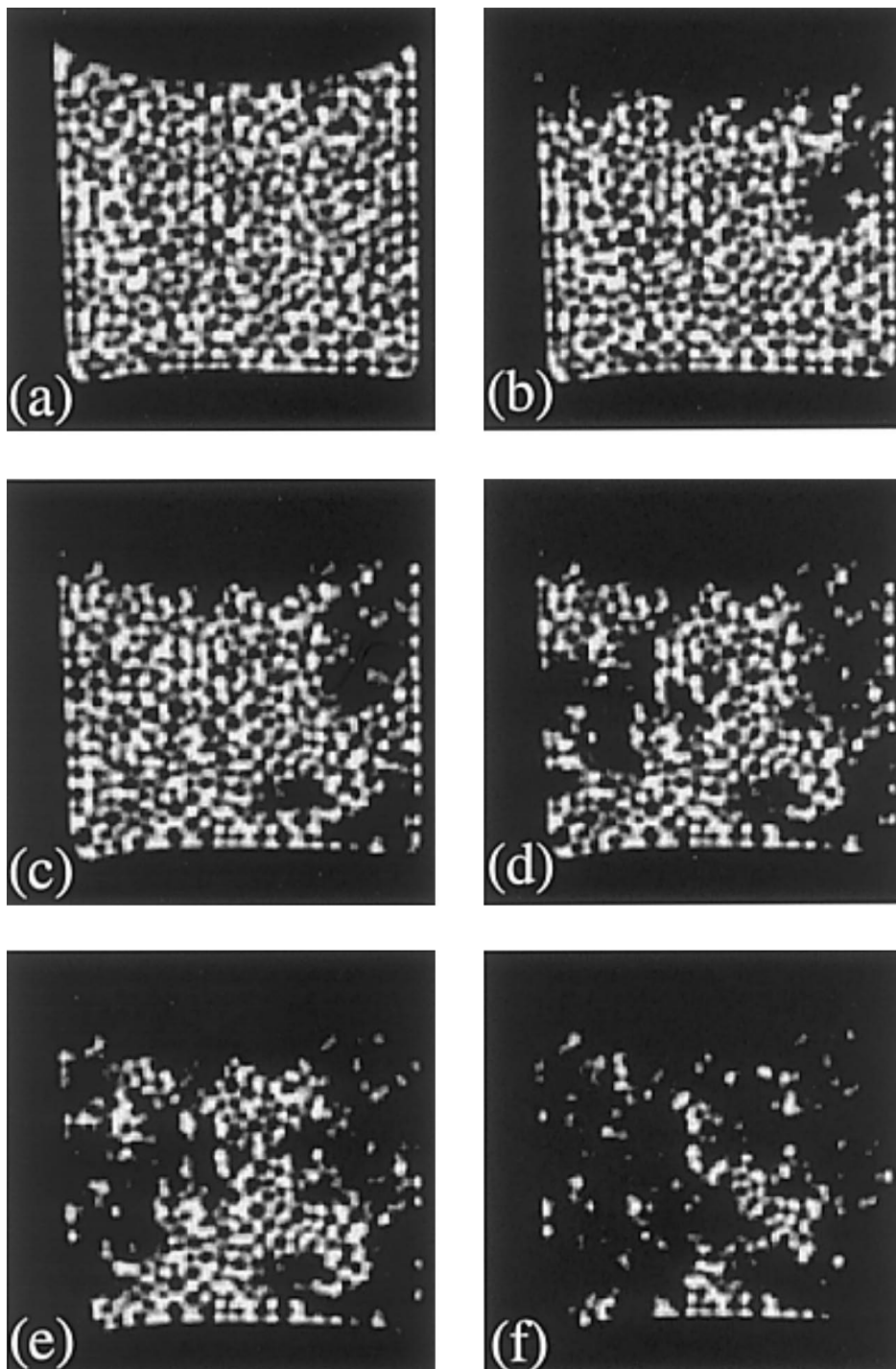


FIG. 4. A series of slices through three-dimensional images obtained with the PEPI hybrid sequence. The sample was a packed bed of 0.5-mm glass spheres inside a 10-mm-diameter glass tube initially filled with deionized water. The voxel resolution is $94\ \mu\text{m}$. The initial water distribution in the pore space is shown in (a). The subsequent images show the water distribution at later times: 1.5 h (b), 3 h (c), 4.25 h (d), 5.25 h (e), and 7 h (f) after acquisition of (a). The inhomogeneous evaporation of the water is clearly visible.

images in Figs. 3a, 3b and 3e, 3f is excellent, while in Fig. 3c severe artifacts appear due to rf pulse errors.

Having demonstrated the three-dimensional PEPI hybrid, the method was then applied to monitor the process of drying within an initially water-saturated model porous medium. This

experiment was part of a larger study, the results of which will be published elsewhere. The model porous medium was a packing, of length 15 mm, of glass spheres of diameter 0.5 mm contained within a 10-mm-diameter glass tube. The pore space was filled with deionized water. The top end of the tube was

open, and air was allowed to circulate around the tube, giving a controlled evaporation of the water. In Fig. 4 images of the water distribution obtained using the three-dimensional PEPI hybrid are shown at different times. It is clearly visible that the drying process is inhomogeneous.

We have demonstrated that the PEPI technique with a microscopic resolution can be implemented on a standard spectrometer, without the need for any hardware modifications. Errors in the rf field can be compensated using a train of composite rf pulses. We have also shown that this technique can be applied to investigate porous media, in which changes are occurring on a time scale not accessible with the spin-echo technique.

ACKNOWLEDGMENTS

B. Manz and P. S. Chow thank Unilever and the Cambridge Commonwealth Trust, respectively, for financial support. L. F. Gladden thanks EPSRC for the award of the NMR spectrometer.

REFERENCES

1. C. A. Baldwin, A. J. Sederman, M. D. Mantle, P. Alexander, and L. F. Gladden, Determination and characterization of the structure of a pore space from 3D volume images, *J. Colloid Interface Sci.* **181**, 79 (1996).
2. L. F. Gladden and P. Alexander, Applications of nuclear magnetic resonance imaging in process engineering, *Meas. Sci. Technol.* **7**, 423 (1996).
3. P. Mansfield, Multi-planar image formation using NMR spin echoes, *J. Phys. C: Solid State Phys.* **10**, L55 (1977).
4. D. N. Guilfoyle, P. Mansfield, and K. J. Packer, Fluid flow measurement in porous media by echo-planar imaging, *J. Magn. Reson.* **97**, 342 (1992).
5. A. M. Peters, P. S. Robyr, R. W. Bowtell, and P. Mansfield, Echo-planar microscopy of porous rocks, *Magn. Reson. Imaging* **14**, 875 (1996).
6. D. N. Guilfoyle, B. Issa, and P. Mansfield, Rapid volumetric NMR imaging of fluids in porous solids using a 3D π -EPI (PEPI) hybrid, *J. Magn. Reson. A* **119**, 151 (1996).
7. J. Hennig, Multiecho imaging sequences with low refocussing flip angles, *J. Magn. Reson.* **78**, 397 (1988).
8. K. Oshio, F. A. Jolesz, P. S. Melki, and R. V. Mulkern, T_2 -weighted thin-section imaging with the multislab 3-dimensional RARE technique, *J. Magn. Reson. Imaging* **1**, 695 (1991).
9. F. Hennel, Modification of the Carr-Purcell sequence for single-shot echo-planar imaging, *Magn. Res. Med.* **26**, 116 (1992).
10. T. Gullion, D. B. Baker, and M. S. Conradi, New, compensated Carr-Purcell sequences, *J. Magn. Reson.* **89**, 479 (1990).
11. M. H. Levitt and R. Freeman, Compensation for pulse imperfections in NMR spin-echo experiments, *J. Magn. Reson.* **43**, 65 (1981).